Hydrological Sciences Journal
Publication details, including instructions for authors and subscription information:
http://www.tandfonline.com/loi/thsj20

Atlantic Ocean sea-surface temperatures and regional streamflow variability in the Adour-Garonne basin, France

Abdoul Aziz Oubeidillah [a], Glenn Tootle [a] & Sally-Rose Anderson [a]

[a] Department of Civil and Environmental Engineering, University of Tennessee, Knoxville, Tennessee, 37996, USA

Available online: 16 Mar 2012

To cite this article: Abdoul Aziz Oubeidillah, Glenn Tootle & Sally-Rose Anderson (2012): Atlantic Ocean sea-surface temperatures and regional streamflow variability in the Adour-Garonne basin, France, Hydrological Sciences Journal, DOI:10.1080/02626667.2012.659250

To link to this article: http://dx.doi.org/10.1080/02626667.2012.659250

Atlantic Ocean sea-surface temperatures and regional streamflow variability in the Adour-Garonne basin, France

Abdoul Aziz Oubeidillah, Glenn Tootle and Sally-Rose Anderson

Department of Civil and Environmental Engineering, University of Tennessee, Knoxville, Tennessee 37996, USA
oaziz@utk.edu

Received 1 December 2010; accepted 29 June 2011; open for discussion until 1 October 2012

Editor Z.W. Kundzewicz; **Associate editor** H. Aksoy

Citation Oubeidillah, A.A., Tootle, G. and Anderson, S.-R., 2012. Atlantic Ocean sea-surface temperatures and regional streamflow variability in the Adour-Garonne basin, France. *Hydrological Sciences Journal*, 57 (3), 1–11.

Abstract The identification of Atlantic Ocean (AO) climatic drivers may prove valuable in long lead-time forecasting of streamflow in the Adour-Garonne basin in southwestern France. Previous studies have identified the Atlantic Multidecadal Oscillation (AMO) and the North Atlantic Oscillation (NAO) as drivers of European hydrology. The current research applied the singular value decomposition (SVD) statistical method to AO sea-surface temperatures (SSTs) to identify the primary AO climatic drivers of the Adour-Garonne basin streamflow. Annual and seasonal streamflow volumes were selected as the hydrological response, while average AO SSTs were calculated for three different 6-month averages (January–June, April–September and July–December) for the year preceding streamflow. The results identified a region along the Equator as the probable driver of the basin streamflow. Additional analysis evaluated the influence of the AMO and NAO on Adour-Garonne basin streamflow.

Key words singular value decomposition (SVD); sea-surface temperature (SST); teleconnection; streamflow; hydrology; climate; Adour-Garonne; France

Températures de surface de l'Océan Atlantique et variabilité des débits régionaux dans le bassin Adour-Garonne (France)
Résumé L'identification de déterminants climatiques liés à l'Océan Atlantique peut s'avérer utile dans les prévisions à long terme des débits du bassin Adour-Garonne dans le Sud-Ouest de la France. Des études précédentes ont identifié l'Oscillation Atlantique multidécennale (OAM) et l'Oscillation Nord Atlantique (ONA) comme déterminants de l'hydrologie européenne. L'étude présente une application de la méthode statistique de décomposition en valeurs singulières (DVS) sur les températures de surface de l'océan Atlantique (TSM), pour identifier les principaux déterminants climatiques de l'océan Atlantique l'écoulement du bassin Adour-Garonne. Les volumes d'écoulement annuels et saisonniers ont été sélectionnés comme réponse hydrologique, et la moyenne des SST de l'océan Atlantique a été calculée pour trois périodes différentes de 6 mois (Janvier à Juin, Avril à Septembre et Juillet à Décembre) pour l'année précédant le débit. Les résultats permettent d'identifier une région le long de l'équateur comme déterminant probable de l'écoulement du bassin. Une analyse supplémentaire a évalué l'influence de l'OAM et du ONA sur le débit du bassin Adour-Garonne.

Mots clefs décomposition en valeurs singulières (DSV); température de surface de la mer (TSM); téléconnexion; débits; hydrologie; climat; Adour-Garonne; France

1 INTRODUCTION

The Adour-Garonne basin is the fifth largest French watershed with an area of 116 000 km^2 (Fig. 1). The main river in the basin is the Garonne River, the third largest in France based on annual flow rate. Approximately 6.5 million people, a tenth of the total French metropolitan population, rely on its water for domestic, agricultural and industrial use with the demand increasing annually.

This basin is dominated by the Pyrenees and Massif Central mountains. The basin's hydrological system is fed by the Garonne and Adour rivers, which originate from the Pyrenees mountain ranges. The Tarn, Lot, Dordogne and Charente rivers all flow from

ISSN 0262-6667 print/ISSN 2150-3435 online

http://dx.doi.org/10.1080/02626667.2012.659250
http://www.tandfonline.com

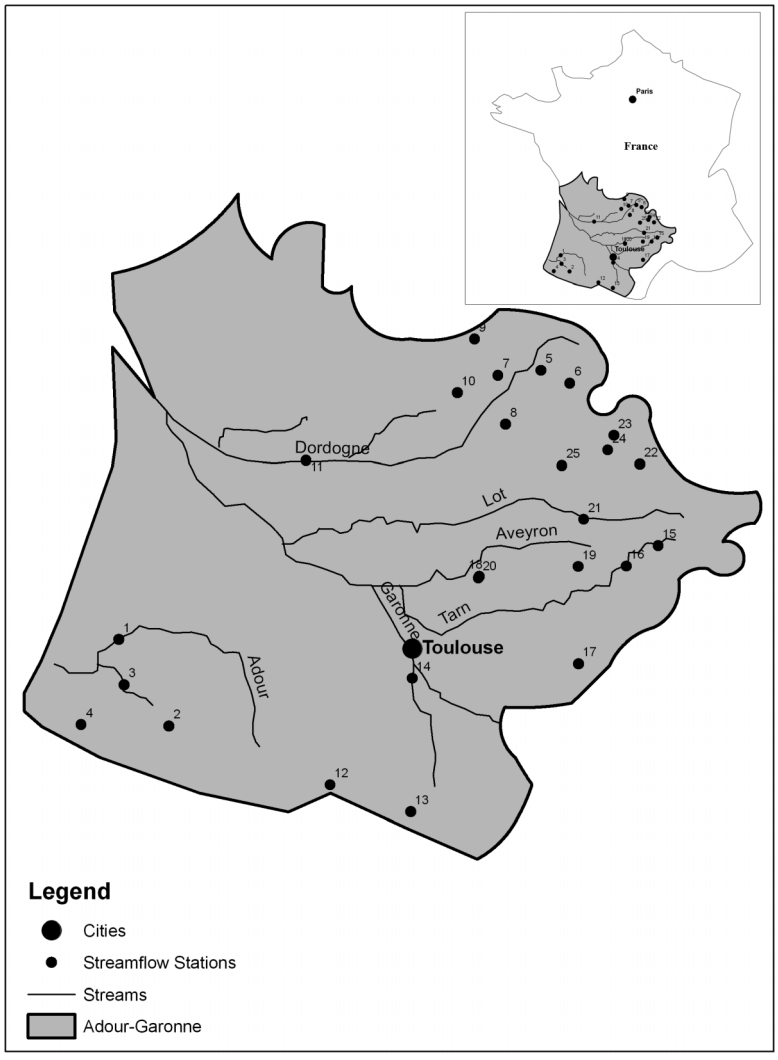

Fig. 1 Map of the Adour-Garonne Basin with locations of streamflow stations. The numbers correspond to those in Table 1.

the Massif Central mountain range. An identification and understanding of any underlying Atlantic Ocean climatic driver will benefit the water availability prediction and management for this region.

A number of studies have evaluated oceanic–atmospheric variability and continental USA hydrological response (e.g. streamflow, precipitation and snowpack) (Cayan and Peterson 1989, Cayan and Webb 1992, Kahya and Dracup 1993, Gershunov 1998, Cayan *et al*. 1999, Enfield *et al*. 2001, McCabe and Dettinger 2002, Rogers and Coleman 2003, Tootle *et al*. 2005, Hunter *et al*. 2006), as well as European hydrology (Rodwell *et al*. 1999, Gallego *et al*. 2005, Massei *et al*. 2007, Lopez-Bustins *et al*. 2008, Bartolini *et al*. 2009, Jacobeit *et al*. 2009, Lavers *et al*. 2010, Brandimarte *et al*. 2011). The papers cited above represent a small number of the many research studies conducted in the area.

The results led to the use of climatic variables as a predictor in long lead-time streamflow forecast models (Uvo *et al*. 2002, Tootle and Piechota 2004, Grantz *et al*. 2005, Pagano and Garen 2006, Tootle *et al*. 2007, Soukup *et al*. 2009). Previous studies evaluating the relationship between the Atlantic Multidecadal Oscillation (AMO) and North Atlantic Oscillation (NAO) climate indices and hydrological response neighbouring regions to the Adour-Garonne basin were inconclusive.

Durand *et al*. (2009) used the French model SAFRAN, which simulates atmospheric conditions related to snowpack, to study the evolution of snowpack given the elevation and slope in the French Alps and Pyrenees. They could not establish a relationship between the NAO and El Niño-Southern Oscillation (ENSO) and snow cover in the French Alps and Pyrenees. Massei *et al* (2007) used continuous

wavelet transforms of seven precipitation time series and compared them with NAO wavelet transforms. They could not establish a link between NAO and rainfall as precipitation records did not contain easily retrievable NAO-like components in northwestern France. Lespinas *et al*. (2010) identified an NAO influence on precipitation; however, it was not strong enough to influence long-term trends in their study of rivers in southern France.

All the study areas in the work cited above were adjacent to the Adour-Garonne basin. Because of its hydrological importance, numerous studies have been conducted to investigate climate change impacts on this region's hydrology (Voirin-Morel 2003, Caballero *et al*. 2007, Hau 2008, Tisseuil 2009).

Bretherton *et al*. (1992) concluded that the singular value decomposition (SVD) approach was simple to use and preferable for general use, while Wallace *et al*. (1992) found that SVD was a powerful technique that isolates the most important modes of variability. Various studies have used SVD to evaluate sea-surface temperature (SST) and hydrological variability (Uvo *et al*. 1998, Enfield and Alfaro 2000, Giannini *et al*. 2000, Wang and Ting 2000, Rajagopalan *et al*. 2000, Rodriguez-Fonseca and de Castro 2002, Martin *et al*. 2004, Shabbar and Skinner 2004, Tootle and Piechota 2006, Tootle *et al*. 2008, Aziz *et al*. 2010). These studies investigated SST and hydrological (e.g. snowpack, drought, precipitation, streamflow) response in the USA, Canada and Europe. While the use of principal components analysis (PCA) is very common in this type of analysis, SVD has the advantage of being able to evaluate the cross-covariance matrix of two spatial–temporal fields to identify similarities between them. In contrast, PCA evaluates only one spatial–temporal field. Additionally, the use of SVD with SSTs and streamflow eliminates the limitations associated with using pre-defined SST regions (e.g. AMO) of climate variability and the resulting streamflow response to phases (e.g. warm or cold) of these climate signals.

Therefore, the hypothesis of the current research is that an Atlantic Ocean SST region (or regions) exist which is a climatic driver of Adour-Garonne basin streamflow. The most well established and understood Atlantic Ocean climate phenomena, AMO and NAO, were not identified as being teleconnected with regions adjacent to the Adour-Garonne basin in previous research efforts. Thus, the identification of an Atlantic Ocean SST climatic driver of Adour-Garonne basin streamflow would represent an important discovery. The motivation of the current research is that the Atlantic Ocean SST region (or regions) identified may be used as a long lead-time predictor of Adour-Garonne basin streamflow. Similar to the Niño 3.4 index representing the ENSO, an index can be developed for the Atlantic Ocean SST region (or regions) identified and this index may be used as a predictor in a statistically based long lead-time streamflow forecast model.

The current research aimed to provide a comprehensive—i.e. three Atlantic Ocean SST (predictor) periods and two Adour-Garonne basin streamflow (predictand) periods—first-time analysis of Atlantic Ocean SSTs and the Adour-Garonne basin streamflow variability and the identification of Atlantic Ocean SST regions that influence streamflow. This study applied SVD to Atlantic Ocean SSTs and Adour-Garonne basin streamflow in an attempt to identify climatic drivers and, perhaps, a useful long lead-time predictor of streamflow. Although not previously identified as a climatic driver of hydrological response in neighbouring regions to the Adour-Garonne basin, an evaluation of Adour-Garonne basin streamflow and climate indices (AMO and NAO) was also performed and compared to previous research efforts. While previous publications evaluated the impact of climate change on water resources of the Adour-Garonne basin (Lehenaff 2002, Caballero *et al*. 2003, 2007), this study focused solely on the possible teleconnection between the Atlantic Ocean SSTs and the regional streamflow.

2 DATA

Atlantic Ocean sea-surface temperature (SST) data were obtained from the National Climatic Data Center website. The National Oceanic and Atmospheric Administration (NOAA) extended reconstructed SST Version 3b from Smith *et al*. (2008) were downloaded from http://www.esrl.noaa.gov/psd/data/gridded/data.noaa.ersst.html. These data consist of a 2° × 2° grid of average monthly SSTs from January 1854 to February 2010. For this study, the SST region spanning 20°S–70°N and 80°W–2°W was used. After land masses were removed, this resulted in 1361 SST cells being identified. Average Atlantic Ocean SSTs were calculated for three different 6-month periods: January–June (JFMAMJ), April–September (AMJJAS) and July–December (JASOND). The period of record for the SSTs is 1960–2005 (46 years).

Streamflow data were obtained from the hydrology website of the Ministry of Ecology and Sustainable Development (Ministère de l'Ecologie

Table 1 List and description of streamflow stations. The numbering corresponds to the station numbers shown on the figure maps.

Station order	Station no.	Station name	Lat*	Lon*	Department
1	Q3120010	L'Adour à Saint-Vincent-de-Paul	1862643	326445	Landes (40)
2	Q7002910	Le Gave d'Oloron à Oloron-Sainte-Marie [Oloron-SN]	1804085	360293	Pyrénées-Atlantiques (64)
3	Q7412910	Le Gave d'Oloron à Escos	1832099	329975	Pyrénées-Atlantiques (64)
4	Q9164610	La Nive des Aldudes à Saint-Étienne-de-Baïgorry	1804972	300932	Pyrénées-Atlantiques (64)
5	P0190010	La Dordogne à Bort-les-Orgues	2045815	612807	Corrèze (19)
6	P0364010	La Santoire à Condat [Roche-Pointue]	2037176	632571	Cantal (15)
7	P1154010	La Luzège à Lamazière-Basse [Pont de Bouyges]	2042504	583744	Corrèze (19)
8	P1502510	La Maronne à Pleaux [Enchanet]	2009197	588829	Cantal (15)
9	P3021010	La Vézère à Bugeat	2067161	567826	Corrèze (19)
10	P3502510	La Corrèze à Tulle [Pont des soldats]	2030679	556281	Corrèze (19)
11	P5140010	La Dordogne à Bergerac	1984849	453459	Dordogne (24)
12	O0015310	Le Maudan à Fos	1764001	469828	Haute-Garonne (31)
13	O1115010	L'Artigue à Auzat [Cibelle]	1745647	524405	Ariège (09)
14	O1900010	La Garonne à Portet-sur-Garonne	1836493	525406	Haute-Garonne (31)
15	O3121010	Le Tarn à Montbrun [Pont de Montbrun]	1926545	692591	Lozère (48)
16	O3141010	Le Tarn à Mostuéjouls [La Muse]	1912540	670860	Aveyron (12)
17	O4102510	L'Agout à Fraisse-sur-Agout	1846445	638444	Hérault (34)
18	O5292510	L'Aveyron à Laguépie [1]	1905684	570939	Tarn-et-Garonne (82)
19	O5344010	Le Vioulou à Salles-Curan [Trébons-Bas]	1912229	638138	Aveyron (12)
20	O5572910	Le Viaur à Laguépie	1904680	570581	Tarn-et-Garonne (82)
21	O7131510	Le Lot à Lassouts [Castelnau]	1944600	642030	Aveyron (12)
22	O7272510	La Truyère au Malzieu-Ville [Le Soulier]	1982106	680007	Lozère (48)
23	O7354010	La Lander à Saint-Georges	2001559	662432	Cantal (15)
24	O7502510	La Truyère à Neuvéglise [Grandval]	1991614	658173	Cantal (15)
25	O7635010	La Bromme à Brommat [EDF]	1981284	627222	Aveyron (12)

* Lambert II coordinate system (France).

et du Developpment Durable) at http://www.hydro.eaufrance.fr. Streamflow time series in this database are produced by regional services called DIREN. For this study, unimpaired streamflow stations (stations identified with no anthropogenic influences) were selected. While there were many streamflow stations with records extending further back in time, many had large gaps of missing data or were discontinued in recent times. Only streamflow stations with complete records were evaluated. The selected period of record for streamflow (1960–2006) balanced the number of stations that had complete records with an acceptable length of record. This resulted in 25 streamflow stations being used in the current research (Table 1).

An evaluation of the distribution of monthly streamflow identified that the period of November to March resulted in the highest streamflow (Fig. 2). This was confirmed by other studies such as Caballero *et al*. (2007), which identified the July–October period as the low-flow period. Thus, streamflow for the November–March period along with the calendar year period were evaluated in the study. Average monthly streamflow rates (in m^3/s) were converted

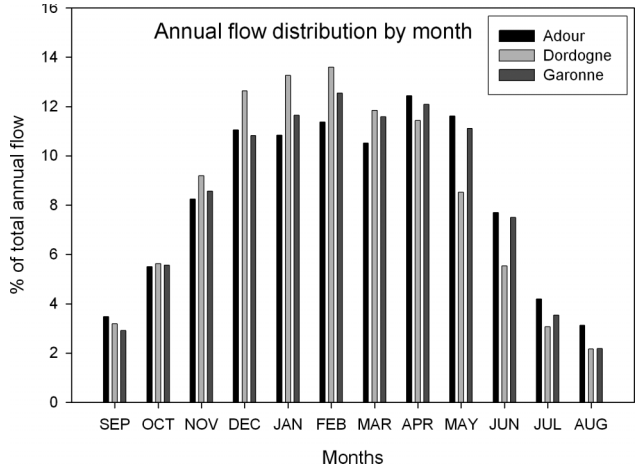

Fig. 2 Monthly distribution of streamflow for the Adour, Dordogne and Garonne rivers in the Adour-Garonne basin as a percentage of total annual flow.

to either calendar year streamflow volume or seasonal (November–March) streamflow volume. Two data sets of 25 streamflow station data were created; the first consisted of annual streamflow volume (in 10^6 m^3/s, or MCM) from January–December of the same year, and the second of streamflow volume (10^6 m^3/s) for November of the previous year to March of the current year. This resulted in a wide range of lead times varying from 0 to 6 months.

The anomalies of the data sets were calculated. For the Atlantic Ocean SSTs, the deviation of the seasonal means from the long time average were calculated for each cell, and for the streamflow, the anomalies were calculated for each station. Each of the data sets was then standardized. These standardized anomalies of the data sets were used in this study. These data sets were then detrended by removing the best straight line fit from the data vectors. Consequently, the correlation results will be independent of any trend that may be present in the data sets.

The Atlantic Ocean oceanic–atmospheric climatic phenomena data used in this study were the Atlantic Multidecadal Oscillation (AMO) and the North Atlantic Oscillation (NAO). The AMO, is an oscillation observed in the northern part of the Atlantic Ocean with long-duration periods that last between 20 and 40 years. It is composed of a cold phase and a warm phase. It is acknowledged to affect air temperature and precipitation over North America and Europe and its footprint can also be identified in Atlantic hurricane frequency data (Enfield *et al*. 2001). The AMO data used in the analysis are the unsmoothed time series from the Kaplan SST Version 2 calculated at NOAA/ESRL/PSD1 and obtained from http://www.cdc.noaa.gov/Pressure/Timeseries/Data/amo.long.data.

The NAO is a winter climate variability defined as the normalized difference in sea-level atmospheric pressure between stations in Iceland and in the Azores. An extended version of the NAO index can be derived by using a station at the southwest part of the Iberian Peninsula (Hurrell 1995). The NAO is also known to affect Atlantic hurricane strength and direction. The data used in this analysis were obtained from http://www.esrl.noaa.gov/psd/gcos_wgsp/Timeseries/Data/nao.long.data.

The average monthly values for the climatic indices (AMO and NAO) were averaged for each of the 6-month (JFMAMJ, AMJJAS, JASOND) predictor periods for the same period of record (1960–2005) as the Atlantic Ocean SSTs.

3 METHODS

3.1 Correlation of streamflow data with AMO and NAO seasonal indices

To evaluate the relationship between the streamflow stations and the Atlantic Ocean climate indices AMO and NAO, simple correlation analyses were performed. The seasonal (JFMAMJ, AMJJAS, JASOND) average values of the climate indices were evaluated with all streamflow stations using Pearson correlation. Thus, the relationship is limited to a pre-determined region of the Atlantic Ocean. To eliminate this limitation, SVD was used to evaluate the relationship between the Atlantic Ocean SST region covering the area between 20°S–70°N and 80°W–2°W and streamflow.

3.2 Singular value decomposition (SVD)

While Bretherton *et al*. (1992) provides a detailed discussion of SVD methods, in the current research, SVD was used in the form:

$$(\boldsymbol{U}, \boldsymbol{S}, \boldsymbol{V}) = \text{svd}(\boldsymbol{X}) \tag{1}$$

This results in a diagonal matrix, $\boldsymbol{S}$, of the same dimension as $\boldsymbol{X}$. The diagonal elements of $\boldsymbol{S}$ were non-negative and were arranged in decreasing order. It also produces the unitary matrices, $\boldsymbol{U}$ and $\boldsymbol{V}$ which were orthogonal singular vectors and were called Left and Right, respectively. The matrices $\boldsymbol{U}$, $\boldsymbol{S}$ and $\boldsymbol{V}$ were such that:

$$\boldsymbol{X} = \boldsymbol{U} \times \boldsymbol{S} \times V^{-1} \tag{2}$$

The matrix $\boldsymbol{X}$ ($m \times n$) with $m \geq n$, was the cross-covariance matrix created from the two spatial–temporal matrices used for the analysis. The matrices must have the same temporal size, while the spatial elements may vary. The matrices can be square or diagonal and it is important to note that the two spatial–temporal fields must consist of detrended standardized anomalies.

In this study, **sst**(x,t) was the left-side matrix composed of x SST anomaly data points over a period T, and $Q(y,t)$ was the right-side matrix composed of y streamflow stations, Q anomalies over the same length period T, with x and y representing the space and t the time. The cross-covariance matrix, $\boldsymbol{X}$, was obtained by multiplying the left-side matrix by the transpose of

the right-side matrix and dividing the product by the number of years.

$$\boldsymbol{X} = \frac{\text{sst} \times \boldsymbol{Q}^{-1}}{T} \tag{3}$$

The modes were determined by the square covariance fractions (SCF) matrix, which was analogous to the eigenvalues in principal components analysis (PCA). The SCF matrix was obtained by dividing each squared element, k of S_k by the sum of all squared elements, arranged in descending order:

$$\text{SCF} = \frac{S_k^2}{\sum S_k^2} \tag{4}$$

Each value indicates a mode and the amount of variance explained in the corresponding mode, with the first mode accounting for the largest percentage of the variation and the second mode accounting for the second-most variation, and so on. All the modes were uncorrelated. The second mode was orthogonal to the first mode which was orthogonal to the third mode, and so on. The temporal expansion series (TES), also known as time series, were analogous to the principal components scores in PCA, and were obtained by projecting the data matrix (left side, right side) into each eigenvector of the corresponding unitary matrix (Left, Right). Consider the Left singular vectors, $\boldsymbol{L}_k$ and the left-side matrix $\mathbf{sst}(x,t)$. The left temporal expansion series (LTES) (A_k) results from:

$$A_k = \boldsymbol{L}_k \times \mathbf{sst}(x,t) \tag{5}$$

The procedure was the same for the right temporal expansion series ($\boldsymbol{B}_k$).

The temporal expansion series were then used to create heterogeneous correlation maps by correlating each time series to the opposing side data set. The following is an example for a left heterogeneous correlation:

$$r_k = \text{r}[\mathbf{sst}(x,t), \boldsymbol{B}_k] \tag{6}$$

Single value decomposition has been shown to detect correlations in data, even when the data set has significant "noise". The terms Left and Right were arbitrarily used for easier comprehension. Interchanging them at the beginning or using different nomenclature would be of no consequence to the results.

4 RESULTS

4.1 Correlations with Atlantic Ocean climate indices

4.1.1 AMO Correlation of the AMO index and streamflow, for the various seasons and lead-times, did not result in a consensus statistical relationship as few streamflow stations were identified as significant at 90% level ($p < 0.1$). When using calendar year streamflow as the predictand, nine (of 25) streamflow stations were significant for the first predictor period (JFMAMJ), seven for the second predictor period (AMJJAS) and nine for the third predictor period (JASOND). As may be seen in Table 1, five stations—Q7002910 (2), O1900010 (14), O7272510 (22), O7354010 (23) and O7502510 (24)—were found to be significant for all three periods. For the November–March streamflow period, fewer streamflow stations were identified as significant. One station was significant for the first predictor period (JFMAMJ) and one station was significant for the second predictor period (AMJJAS). The JASOND was not correlated due to overlap with the predictand period (November–March). The streamflow stations that displayed statistical significance with the AMO exhibited a negative correlation. Thus, a positive phase of the AMO results in a decrease in streamflow in the region, and *vice versa*.

4.1.2 NAO Correlation of the NAO index was similar to that of the AMO index. Eight annual streamflow stations were significant for the first (JFMAMJ) period, five for the second (AMJJAS) period, and zero for the third (JASOND) period. When using the November–March streamflow, only five stations were significant for the first (JFMAMJ) and none were significant for the second (AMJJAS) predictor period. The JASOND period was not correlated due to overlap with the predictand period (November–March).

The streamflow stations that showed a significant correlation with the NAO exhibited a negative relationship; thus, a positive phase of the NAO results in a decrease in streamflow in the region, and *vice versa*. Interestingly, Hurrell (1995) identified a similar finding on the correlation between euro-Mediterranean region precipitation and the NAO. Struglia *et al*. (2004) found similar negative correlations between the NAO and streamflow stations discharging into the Mediterranean Sea, which include stations adjacent to the Adour-Garonne region. Given the lack of an AMO or NAO climate signal in the Adour-Garonne

basin streamflow, it is highly unlikely that these established climate signals, when used in a long lead-time statistical streamflow forecast model, will produce acceptable (skilful) results.

4.2 SVD analysis

The cumulative SCF for the first three modes was above 90% in all cases. Generally, if the leading three modes explain a significant (greater than 80%) amount of the variance between the two fields, then SVD can be applied to determine the strength of the coupled variability present (Newman and Sardeshmukh 1995). Therefore, SVD can be applied in the current research efforts.

The results of this study show that the majority of the variability in the data is explained in the first mode. The first mode square covariance fractions (SCF) ranged from 75% to 85%. Given the vast majority of the variability was explained in the first mode, only figures for the first mode were provided.

4.2.1 Annual streamflow For the annual streamflow, the cumulative square covariance fractions, for the first three modes, for the three SST predictor periods (JFMAMJ, AMJJAS and JASOND) were 94, 95 and 96%, respectively (Fig. 3).

For the first period (JFMAMJ) Atlantic Ocean SSTs, 22 out of the 25 stations were significant at 90% for the first mode (first mode SCF = 85%). The streamflow correlation values were positive (see Fig. 3, right panel): 524 of the 1361 SST cells were significant at 90% in the first mode. The significant SST cells are in a region along the Equator between Brazil and Senegal, and the eastern Atlantic near northwest Africa. A small region just east of North America, almost centred at 30°N, 15°W, was also identified. All of the SST correlation values were negative (see Fig. 3, left panel). In SVD, the opposite signs identified in the streamflow stations and SST regions reveal that they behave in an opposite manner. When the significant Atlantic Ocean SSTs regions identified increase in temperature, the significant Adour-Garonne basin streamflow stations identified decrease in runoff volume, and *vice versa*.

For the second period (AMJJAS) Atlantic Ocean SSTs, 23 of the 25 streamflow stations were identified as 90% significant and displayed a positive relationship (Fig. 3, right) in the first mode (first mode SCF = 88%). Non-significant streamflow stations observed in this period were similar to those identified in the first period. An SST region, similar to the one identified in the first period, was identified. However, the small region east of North America shifted slightly north. In all, about 600 SST cells exhibited negative correlation (Fig. 3, left).

Results from the third 6-month period (JASOND) Atlantic Ocean SSTs were almost identical to the second period results in that 23 of the 25 streamflow stations were 90% significant and displayed a positive relationship (Fig. 3, right) in the first mode (first mode SCF = 89%). The identified Atlantic Ocean SST region exhibited a similar pattern as the first two SST predictor periods with a region extending down the west coast of Europe and Africa and along the Equator between Brazil and Africa. In addition, the SST pattern spanned across the Atlantic Ocean, linking the previously identified region east of North America with the region along the west coast of Europe just above the 30th parallel, covering the Azores islands. In all, about 600 SST cells had negative correlation values (Fig. 3, left).

4.2.2 November–March streamflow For this period, the cumulative square covariance fractions for the three periods (JFMAMJ, AMJJAS and JASOND) were 92, 93 and 93%, respectively (Fig. 4).

For the first period (JFMAMJ) Atlantic Ocean SSTs, 20 of the 25 stations were significant at 90% for the first mode (first mode SCF = 77%). The streamflow correlation values were positive (Fig. 4, right panel). Approximately 300 of the 1361 SST cells were significant at 90% in the first mode and had negative correlation values (Fig. 4, left panel). The significant SST cells are in a region along the Equator between Brazil and Senegal, a small region of the east coast of North America and a region northwest of Europe.

For the second period (AMJJAS) Atlantic Ocean SSTs, 20 of the 25 streamflow stations were identified as 90% significant in the first mode (first mode SCF = 74%). The streamflow correlation values were positive (Fig. 4, right). Similar non-significant streamflow stations observed in the first period were also not significant in the second period. An SST region similar to the one observed in the first period was also identified. In addition, another SST region covering the Azores islands, just above the 30th parallel, was also observed. In all, about 300 SST cells had negative correlation values (Fig. 4, left).

The third SST period (JASOND) was not evaluated because it overlapped with the predictand period.

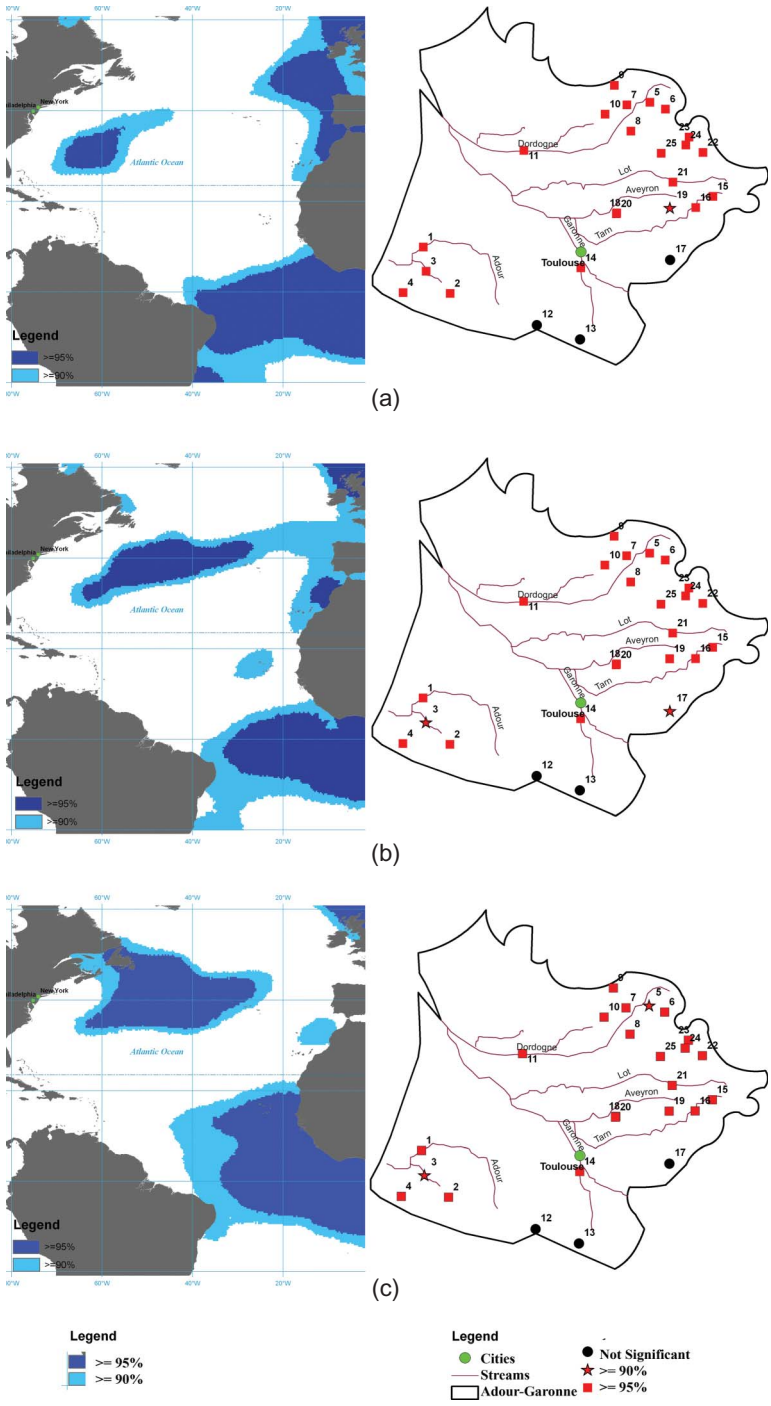

Fig. 3 Heterogeneous correlation figures (first mode) for: (a) JFMAMJ, (b) AMJJAS and (c) JASOND when applying SVD to the previous year Atlantic Ocean SSTs (left), and current year (January–December) streamflow (right).

5 DISCUSSION AND CONCLUSIONS

The results identified no clear relationship between established Atlantic Ocean climate indices (AMO, NAO) and streamflow in the Adour-Garonne basin, which confirmed previous research in adjacent regions. As a result of the eight subsequent evaluations of Atlantic Ocean SSTs and Adour-Garonne basin streamflow detailed above, it appears that the streamflow in the Adour-Garonne basin is influenced by Atlantic Ocean SSTs along the equatorial region between Brazil and the west coast of Africa, and a region off the west coast of Europe.

As discussed above, it is important to note the nature of the relationship between the Atlantic Ocean

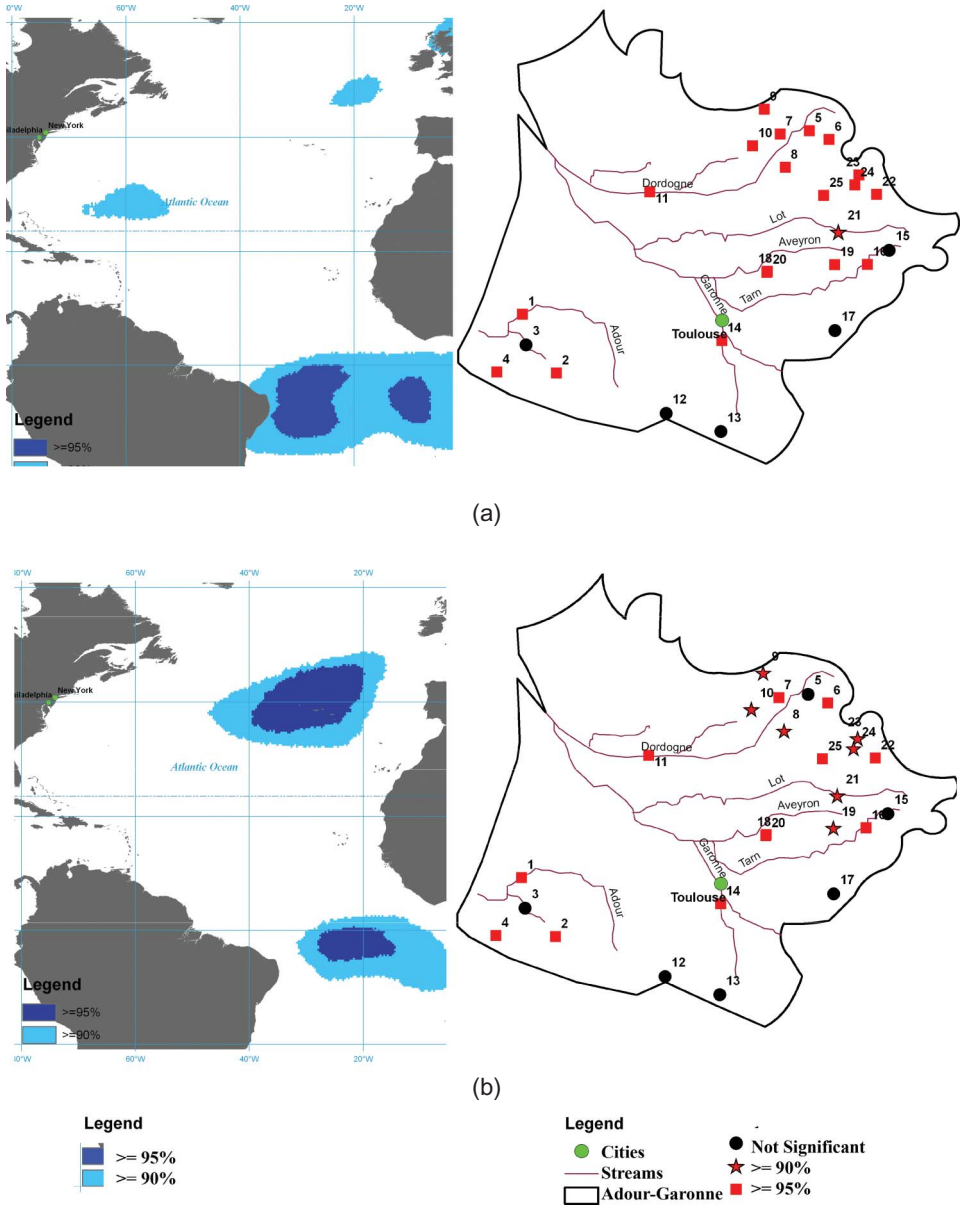

Fig. 4 Heterogeneous correlation figures (first mode) for: (a) JFMAMJ and (b) AMJJAS, and seasonal (November–March) when applying SVD to the previous year Atlantic Ocean SSTs (left) and streamflow (right).

SST regions and the Adour-Garonne basin streamflow stations by observing the signs of the correlation values for each data set. By analysing the resulting data and figures, it was apparent that the identified Atlantic Ocean SST regions and the Adour-Garonne basin streamflow stations have an opposite relationship. This was explained because the SST regions show negative correlation values and the streamflow stations show positive correlations.

For the long lead-time analysis, the majority of higher SST correlation values were consistently concentrated along the Equator. Increasing the lag time between the SST periods and the streamflow period from 0 to 6 months identified a similar Atlantic Ocean SST equatorial region. Interestingly, the signal was stronger (higher correlations) for the longer lag time than for the shorter lag time.

Additionally, an SST time series index was created for the Atlantic Ocean region spanning 10°S to 4°N and 30°W to 2°W, by taking the annual average of all the cell SSTs within that region. This time series was then correlated to each streamflow station. All but five stations resulted in significant correlation (r) values ranging from −0.26 to −0.49. It is

interesting to note that the correlation test shows a negative relationship similarly to the SVD analysis results.

Future research may focus on the use of a non-parametric or regression-based long lead-time streamflow forecast model (Hastenrath *et al*. 1984, Tootle and Piechota 2004, Tootle *et al*. 2007, Soukup *et al*. 2009) for Adour-Garonne basin streamflow. Additionally, future research efforts may focus on determining a physical explanation of the results (Atlantic SST regions identified) found in this study by examining z500 geopotential height winds as well as global circulation phenomena. Li (2000) stated that the physical mechanisms affecting the inter-annual and inter-decadal climate variability in the tropical Atlantic Ocean are not yet understood. The paper also identified two modes of variability, and the one centred in the equatorial region with ENSO-like dynamics involving the thermocline depth of the Ocean and the atmosphere's trade winds, could be responsible. Similar results were found by Chang *et al*. (1997), who also pointed out that the equatorial region of the Atlantic SST has been found in many studies to influence the variability of Northeast Brazil and Sahel rainfall (Moura and Shukla 1981, Hastenrath 1984, Follan *et al*. 1986).

Acknowledgements The authors wish to thank Christian Viel of the Production Department at Météo-France for his outstanding support and suggestions. The authors would also like to extend their appreciation to the Ministère de l'Ecologie et du Developpment Durable for granting access to the HYDRO database. The research is supported by the University of Tennessee, Knoxville and Oak Ridge National Laboratory Joint Directed Research and Development (JDRD) program and the National Science Foundation P2C2 award AGS-1003393.

REFERENCES

Aziz, O.A. *et al*., 2010. Identification of Pacific Ocean sea surface temperature influences of the Upper Colorado River Basin snowpack. *Water Resources Research*, 46, W07436.

Bartolini, E. *et al*., 2009. Interannual variability of winter precipitation in the European Alps: relations with the North Atlantic Oscillation. *Hydrology and Earth System Sciences*, 13 (1), 17–25.

Brandimarte, L. *et al*., 2011. Relation between the North-Atlantic Oscillation and hydroclimatic conditions in Mediterranean areas. *Water Resources Management*, 25 (5), 1269–1279.

Bretherton, C.S., Smith, C. and Wallace, J.M., 1992. An intercomparison of methods for finding coupled patterns in climate data. *Journal of Climate*, 5, 541–560.

Caballero, Y. *et al*., 2007. Hydrologic sensitivity of the Adour-Garonne River basin to climate change. *Water Resources Research*, 43, W07448.

Caballero, Y. and Noilhan, J., 2003. Etude de l'impact hydrologique du changement climatique sur les ressources en eau du bassin Adour Garonne. Toulouse, France: Météo-France.

Cayan, D.R. and Peterson, D.H., 1989. The influence of North Pacific atmospheric circulation on streamflow in the west. *In*: *Aspects of climate variability in the Pacific and the western Americas*. Washington, DC: American Geophysical Union, Geophysical Monograph Series 55, 375–397.

Cayan, D.R. Redmond, K.T. and Riddle, L.G., 1999. ENSO and hydrologic extremes in the western US *Journal of Climate*, 12 (9), 2881–2893.

Cayan, D.R. and Webb, R.H., 1992. El Niño/Southern Oscillation and streamflow in the western United States. *In: El Niño: Historical and paleoclimatic aspects of the Southern Oscillation*. New York: Cambridge University Press.

Chang, P. *et al*., 1997. A decadal climate variation in the tropical Atlantic Ocean from thermodynamic air–sea interactions. *Nature*, 385 (6616), 516–518.

Durand, Y. *et al*., 2009. Reanalysis of 47 years of climate in the French Alps (1958–2005): climatology and trends for snow cover. *Journal of Applied Meteorology and Climatology*, 48, 2487–2512.

Enfield, D.B. and Alfaro, E.J., 2000. The dependence of Caribbean rainfall on the interaction of the tropical Atlantic and Pacific oceans. *Journal of Climate*, 12 (7), 2093–2103.

Enfield, D.B., Mestas-Nuñez, A.M. and Trimble, P.J., 2001. The Atlantic multidecadal oscillation and its relation to rainfall and river flows in the continental US. *Geophysical Research Letters*, 28 (10), 2077–2080.

Folland, C.K. *et al*., 1986. Sahel rainfall and worldwide sea temperatures, 1901–85. *Nature*, 320 (6063), 602–607.

Gallego, M.C. *et al*., 2005. The NAO signal in daily rainfall series over the Iberian Peninsula. *Climate Research*, 29 (2), 103–109.

Gershunov, A., 1998. ENSO influence on influence on intraseasonal extreme rainfall and temperature frequencies in the contiguous United States: implications for long-range predictability. *Journal of Climate*, 11, 3192–3203.

Giannini, A., Kushnir, Y. and Cane, M.A., 2000. Interannual variability of Caribbean rainfall, ENSO, and the Atlantic Ocean. *Journal of Climate*, 13, 297–311.

Grantz, K. *et al*., 2005. A technique for incorporating large-scale climate information in basin-scale ensemble streamflow forecasts. *Water Resources Research*, 41, W10410.

Hastenrath, S., 1984. Interannual variability and annual cycle—mechanisms of circulation and climate in the tropical Atlantic sector. *Monthly Weather Review*, 112 (6), 1097–1107.

Hastenrath, S. *et al*., 1984. Towards the monitoring and prediction of Northeast Brazil droughts. *Quarterly Journal of the Royal Meteorological Society*, 110 (464), 411–425.

Hau, M., 2008, Modélisation hydrologique des sous-bassins versants de la Garonne a l'aide d'un modèle pluie–débit global. Cemagref.

Hunter, T., Tootle, G.A. and Piechota, T.C., 2006. Oceanic–atmospheric variability and western US snowfall. *Geophysical Research Letters*, 33, L13706.

Hurrell, J.W., 1995. Decadal trends in the North Atlantic Oscillation: regional temperatures and precipitation. *Science*, 7, 676–679.

Jacobeit, J. *et al*., 2009. Central European precipitation and temperature extremes in relation to large-scale atmospheric circulation types. *Meteorologische Zeitschrift*, 18 (4), 397–410.

Kahya, E. and Dracup, J.A., 1993. US streamflow patterns in relation to the El Niño / Southern Oscillation. *Water Resources Research*, 29 (8), 2491–2503.

Lavers, D. *et al*., 2010. Large-scale climate, precipitation and British river flows identifying hydroclimatological connections and dynamics. *Journal of Hydrology*, 395 (3–4), 242–255.

Lehenaff, A., 2002. *Impact du changement climatique sur la resource en eau du basin Adour Garonne*. Ecole Nationale de Météorologie, Météo-France, Toulouse.

Lespinas, F., Ludwig, W. and Heussner, S. 2010. Impact of recent climate change on the hydrology of coastal Mediterranean rivers in southern France. *Climatic Change*, 99, 425–456.

Li, Z.X., 2001. Thermodynamic air–sea interactions and tropical Atlantic SST dipole pattern. *Physics and Chemistry of the Earth* Part B – *Hydrology Oceans and Atmosphere*, 26 (2), 155–157.

Lopez-Bustins, J.A. *et al*., 2008. Iberia winter rainfall trends based upon changes in teleconnection and circulation patterns. *Global and Planetary Change*, 63 (2–3), 171–176.

McCabe, G.J. and Dettinger, M.D., 2002. Primary modes and predictability of year-to-year snowpack variations in the western United States from teleconnections with Pacific Ocean climate. *Journal of Hydrometeorology*, 3 (1), 13–25.

Martin, M.L. *et al*., 2004. North Atlantic teleconnection patterns of low-frequency variability and their links with springtime precipitation in the western Mediterranean. *International Journal of Climatology*, 24 (2), 213–230.

Massei, N. *et al*., 2007. Investigating possible links between the North Atlantic Oscillation and rainfall variability in northwestern France. *Journal of Geophysical Research*, 112, D09121.

Moura, A.D. and Shukla, J., 1981. On the dynamics of droughts in Northeast Brazil—observations, theory and numerical experiments with a general-circulation model. *Journal of the Atmospheric Sciences*, 38 (12), 2653–2675.

Newman, M. and Sardeshmukh, P.D., 1995. A caveat concerning singular value decomposition. *Journal of Climate*, 8, 352–360.

Pagano, T.C. and Garen, D.C., 2006. Climate variations, climate change, and water resources engineering. *In: Integration of climate information and forecasts into western US water supply forecasts*. Reston, VA: ASCE Publications, 86–102.

Rajagopalan B. *et al*., 2000. Spatiotemporal variability of ENSO and SST teleconnections to summer drought over the United States during the twentieth century. *Journal of Climate*, 13, 4244–4255.

Rodriguez-Fonseca, B. and de Castro, M., 2002. On the connection between winter anomalous precipitation in the Iberian Peninsula and north west Africa and the summer subtropical Atlantic sea surface temperature. *Geophysical Research Letters*, 29 (18), 10, 1–4.

Rodwell, M.J. *et al*., 1999. Oceanic forcing of the wintertime North Atlantic Oscillation and European climate. *Nature*, 398 (6725), 320–323.

Rogers, J.C. and Coleman, J.S.M., 2003. Interactions between the Atlantic Multidecadal Oscillation, El Niño/La Niña, and the PNA in winter Mississippi Valley stream flow. *Geophysical Research Letters*, 30 (10), 25, 1–4.

Shabbar, A. and Skinner, W., 2004. Summer drought patterns in Canada and the relationship to global sea surface temperatures. *Journal of Climate*, 17, 2866–2880.

Smith, T.M. *et al*., 2008. Improvements to NOAA's historical merged land–ocean surface temperature analysis (1880–2006). *Journal of Climate*, 21, 2283–2296.

Soukup, T., *et al*., 2009. Incorporating climate into a long lead-time non-parametric streamflow forecast. *Journal of Hydrology*, 368 (2009), 131–142.

Struglia, M.V., Mariotti, A. and Fillograsso, A., 2004. River discharge into the Mediterranean Sea: climatology and aspects of the observed variability. *Journal of Climate*, 17, 4740–4751.

Tisseuil, C., 2009. *Modéliser l'impact du changement climatique sur les écosystèmes aquatiques par approche de downscaling*. Thèse de doctorat, Université de Toulouse, France.

Tootle, G.A. and Piechota, T.C., 2004. Suwannee River long-range streamflow forecasts based on seasonal climate predictors. *Journal of the American Water Resources Association*, 40 (2), 523–532.

Tootle, G.A. and Piechota, T.C., 2006. Relationships between Pacific and Atlantic Ocean sea surface temperatures and US streamflow variability. *Water Resources Research*, 42, W07411.

Tootle, G.A., Piechota, T.C. and Gutierrez, F., 2008. The relationships between Pacific and Atlantic Ocean sea surface temperatures and Colombian streamflow variability. *Journal of Hydrology*, 349 (3–4), 268–276.

Tootle, G.A., Piechota, T.C. and Singh, A.K., 2005. Coupled oceanic/atmospheric variability and United States streamflow. *Water Resources Research*, 41, W12408.

Tootle, G.A. *et al*., 2007. Long lead-time forecasting of US streamflow using partial least squares regression. *Journal of Hydrologic Engineering of the American Society of Civil Engineers*, 12 (5), 442–451.

Uvo, C. B. and R. Berndtsson (2002). North Atlantic oscillation; a climatic indicator to predict hydropower availability in Scandinavia. *Nordic Hydrology*, 33 (5), 415–424.

Uvo, C.B. *et al*., 1998. The relationships between tropical Pacific and Atlantic SST and Northeast Brazil monthly precipitation. *Journal of Climate*, 11, 551–562.

Voirin-Morel, S., 2003. *Modélisation distribuée des flux d'eau et d'énergie et des debits à l'échelle régionale du basin Adour Garonne*. Thesis (PhD), University Paul Sabatier, Toulouse III, Toulouse, France.

Wallace, J.M., Gutzler, D.S. and Bretheron, C.S., 1992. Singular value decomposition of wintertime sea surface temperature and 500-mb height anomalies. *Journal of Climate*, 5, 561–576.

Wang, H. and Ting, M., 2000. Covariabilities of winter US precipitation and Pacific sea surface temperatures. *Journal of Climate*, 13, 3711–3719.